RSC Advances

PAPER

View Article Online
View Journal | View Issue

Cite this: *RSC Adv.*, 2018, **8**, 31575

Green fabrication of nanoporous $BiVO_4$ films on ITO substrates for photoelectrochemical water-oxidation†

Sayuri Okunaka,[a] Yutaka Hitomi[b] and Hiromasa Tokudome*[a]

Received 9th July 2018
Accepted 3rd September 2018

DOI: 10.1039/c8ra05831h

rsc.li/rsc-advances

A new green method was developed to prepare nanoporous $BiVO_4$ films on ITO substrates for photoelectrochemical (PEC) water-oxidation under visible light irradiation. The films can be prepared by simple drop-casting of a stable aqueous solution of Bi^{3+} and V^{5+} complexes with tartaric acid and ethylenediaminetetraacetic acid, followed by drying and calcination in air. Thanks to these ligands, the aqueous precursor solution is remarkably stable over a wide range of pH (pH 4–9). The $BiVO_4$ films on ITO substrates possess a 3D-network structure comprised of nanoparticles with a scheelite–monoclinic phase and a diameter of *ca.* <100 nm, after calcination at 450–500 °C for 1 h. The PEC performance clearly depended on the film thickness that can be controlled by coating times, and calcination conditions (temperature and time). The CoPi-loaded $BiVO_4$ electrodes exhibited relatively high performance for PEC water oxidation (ABPE of 0.35% at 0.8 V *vs.* RHE) under simulated sunlight irradiation.

Introduction

Photoelectrochemical (PEC) water splitting using semiconductor photoelectrodes is a promising technology for sustainable energy supply, equal with photocatalytic water splitting using semiconductor particles.[1–4] Development of photoelectrodes that can harvest a wide range of visible light to split water efficiently is indispensable for achieving practically useful conversion of solar energy to H_2. Among various visible-light-responsive photoelectrode materials, $BiVO_4$ (ref. 5) has attracted much attention as an efficient photoanode material that can absorb light up to 520 nm.[6–27] A lot of methods have been reported to fabricate $BiVO_4$ thin films on conducting electrodes. For example, Kim and Choi have reported that nanoporous $BiVO_4$ electrodes can be prepared by applying a DMSO solution of $VO(acac)_2$ onto a surface of electrochemically synthesized BiOI electrodes, and calcining (Fig. S1(a)†).[12] The electrode exhibits high photocurrent (*ca.* 2.7 and 5.0 mA cm^{-2} at 0.60 and 1.23 V *vs.* RHE, respectively) under simulated solar-light irradiation because the nanoporous $BiVO_4$ electrodes have appropriate conductive paths for efficient electron transfer as well as controlled pores allowing efficient reaction and transportation of substances. For practical use, however, it is desired that such a controlled structure is prepared by more facile processes. Various metal oxide thin films are prepared from metal precursors, for example, *via* the sol–gel method.[6,20] However, the metal precursors are generally unstable in aqueous solutions; therefore, organic solvents are commonly used to dissolve corresponding metal sources. The use of organic solvents is an obstacle for industrial processes from the viewpoint of environmental pollution. Therefore, in order to reduce volatilization of organic solvents, the use of water as a solvent has been strongly demanded to widen the range of application and also to reduce the environmental burdens. Recently, it has been reported that $BiVO_4$ photoelectrodes can be prepared by using highly acidic aqueous precursor solutions, although it is also not environmentally friendly (Fig. S1(b)†).[16,17]

We recently found that $BiVO_4$ nanoparticles can be prepared *via* a newly-developed aqueous-chelate method using an aqueous solution of Bi and V ions containing ethylenediaminetetraacetic acid (EDTA) and tartaric acid (tart).[28] In these aqueous solutions, EDTA and tart can serve as good chelators to stabilize Bi and V ions in aqueous solutions at pH 4 to 9. We also found that this new method affords $BiVO_4$ particles with scheelite–monoclinic (s–m) phase, which is known as the most favourable crystal phase for water oxidation reaction, and small particle sizes (<100 nm) and partly networked structures, even after calcination process. These findings have motivated us to apply the precursor aqueous solution of mild pH to the fabrication of $BiVO_4$ photoelectrodes that can efficiently act under visible light. In this study, we have successfully fabricated nanoporous $BiVO_4$ photoanodes *via* the

[a]*Research Institute, TOTO LTD., 2-8-1 Honson, Chigasaki, Kanagawa 253-8577, Japan. E-mail: hiromasa.tokudome@jp.toto.com; Fax: +81 467 54 1185; Tel: +81 467 54 3384*

[b]*Department of Molecular Chemistry and Biochemistry, Faculty of Science and Engineering, Doshisha University, 1-3 Tatara Miyakodani, Kyotanabe, Kyoto 610-0321, Japan*

† Electronic supplementary information (ESI) available: photograph, UV-Vis spectrum, stretching Raman shift, SEM images and photocurrent data. See DOI: 10.1039/c8ra05831h

environmentally friendly water-based method and applied them for PEC water oxidation reaction under visible light.

Experimental

Materials

Ammonium vanadate(V) (NH_4VO_3, 99%) and bismuth(III) nitrate pentahydrate ($Bi(NO_3)_3 \cdot 5H_2O$, 99.9%) were purchased from Kanto Chemical. EDTA, tart and ammonia solution (28.0–30.0%) were purchased from Wako Pure Chemical Industries, Ltd. All reagents were used as received, and all the experiments were carried out under ambient conditions.

Preparation of $BiVO_4$ electrodes by using aqueous solutions containing Bi and V ions

The aqueous precursor solutions containing V and Bi ions were prepared *via* aqueous-chelate method, which was recently developed by our group,[28] as follows; A 10 mL aqueous solution that contains $Bi(NO_3)_3 \cdot 5H_2O$ (0.17 M, 0.82 g), EDTA (0.34 M, 0.99 g) and 28% ammonia solution (10 mM, 1.0 g) was mixed with a 10 mL aqueous solution of NH_4VO_3 (0.17 M, 0.20 g) and tart (0.17 M, 0.25 g). The simple addition of $Bi(NO_3)_3 \cdot 5H_2O$ or NH_4VO_3 to water rapidly form precipitate due to rapid hydrolysis. In contrast, the combinations of $Bi(NO_3)_3 \cdot 5H_2O$ with EDTA, and of NH_4VO_3 with tart produce a transparent aqueous solution. As we previously reported,[28] we confirmed that EDTA and tart make stable complexes with Bi^{3+} and V^{5+} ions in aqueous solution, respectively. $BiVO_4$ electrodes were prepared by drop-casting method as follows; the aqueous precursor solution containing V and Bi ions was diluted seven-fold and then dropped on a cleaned tin-doped indium oxide (ITO) transparent conductive glass substrate. The film was dried at 65 °C for 10 min. The as-prepared films were then calcined at 500 °C for 1 h to yield 1-coated $BiVO_4$ films, which were denoted as 1-coated-500 °C-1 h. Films with more than two coats (*n*-coat) were prepared by repeating drop casting, drying and calcinations. Calcination was conducted basically at 500 °C for 1 hour, while other temperatures (*e.g.* 450 and 550 °C) and calcinations times (*e.g.* 2 and 3 hours) were applied in some cases.

Preparation of CoPi-loaded $BiVO_4$ electrodes

A CoPi was electrochemically deposited on the $BiVO_4$ photoelectrodes according to the literature.[8] The electrolyte was prepared by dissolving 2 mM $Co(NO_3)_2 \cdot 6H_2O$ (Wako, 99.5%) in a 0.2 M potassium phosphate buffers solution (pH 7.0). The potential of the working electrode was controlled by a potentiostat (Hokuto Denko, HZ-7000) with a three-electrode cell consisting of the $BiVO_4$ electrode, a Pt wire and a KCl-saturated Ag/AgCl electrode as the working, counter, and reference electrodes, respectively. The electrodeposition was performed at a constant voltage of 1.1 V *vs.* RHE for 2 min.

Characterization

The resulting $BiVO_4$ fine particles were characterized by means of an X-ray diffraction (XRD, PANalytical, X'Pert Pro, rotating anode diffractometer, 45 kV, 40 mA) with Cu K_α radiation (K_α = 1.5406 Å), a UV-Vis-NIR spectrometer (UV-Vis. DRS, Jasco, V-670), and a scanning electron microscope (SEM, HITACHI, S-4100).

PEC measurements of $BiVO_4$ electrodes

PEC properties were evaluated in potassium phosphate buffers (0.2 M, pH 7.0, 0.1 M K_2SO_4) using a potentiostat with a three-electrode cell consisting of the $BiVO_4$ electrode, a Pt electrode, and a KCl-saturated Ag/AgCl electrode as the working, counter, and reference electrodes, respectively. The working electrode was irradiated from the backside (ITO side) with simulated sunlight (AM 1.5G, 100 mW cm^{-2}).

Results and discussion

Characterization of $BiVO_4$ electrodes fabricated by using aqueous solutions containing Bi and V ions

$BiVO_4$ electrodes were prepared by drop-casting the precursor solution onto ITO transparent conductive glass substrates, followed by drying and calcining at 450–550 °C for 1–3 h. The prepared electrodes were yellow transparent thin films (see Fig. 1, calcined at 500 °C for 1 h for example). The XRD analysis revealed that the electrodes have pure scheelite phase of $BiVO_4$ (JCPDS-ICDD: 14-0688) regardless of calcination conditions. No appreciable peak attributed to impurity phases was observed (Fig. 2). The bandgap estimated from the UV-Vis spectra (Fig. S2†) was *ca.* 2.4 eV, which is characteristic of s–m phase $BiVO_4$.[29] The Raman signal attributed to V–O stretching was observed at around 830 cm^{-1}. The estimated value of V–O bond length (*ca.* 1.69 Å, see Table S1†) is in agreement with the reported value for s–m $BiVO_4$ (1.72 Å).[30] Judging from these results, it can be concluded that all the electrodes consist of s–m $BiVO_4$.

The SEM images of $BiVO_4$ electrodes, which were calcined at 450, 500 and 550 °C for 1–3 hour, are shown in Fig. 3 and S3.† The surface SEM images show nanostructures with particle-networks and pores. The primary particle sizes became larger as increasing calcination temperatures; the samples calcined at 450 and 500 °C consisted of relatively uniform particles with

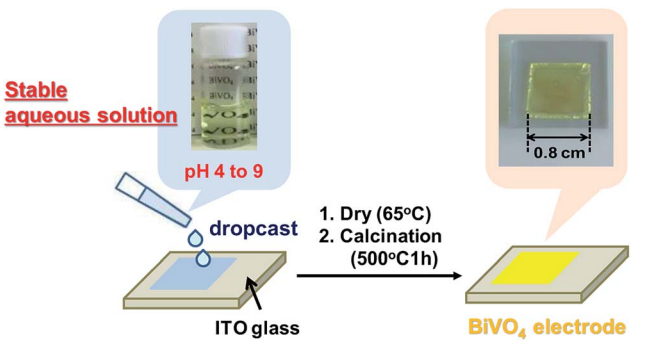

Fig. 1 Fabrication process of a $BiVO_4$ electrode, which was prepared by coating an aqueous Bi and V solution (pH 7) onto an ITO glass substrate (1.25 × 1.25 cm^2), followed by drying (65 °C) and calcination at 500 °C for 1 h.

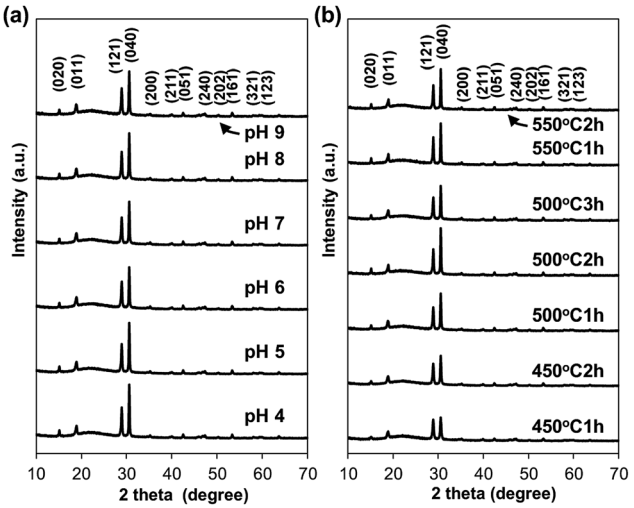

Fig. 2 XRD patterns of $BiVO_4$ electrodes prepared (a) by coating an aqueous precursor solution of various pH (pH 4 to 9) followed by dryness and calcination at 500 °C for 1 h, and (b) by coating an aqueous precursor solution of pH 9 followed by dryness and calcination under different conditions.

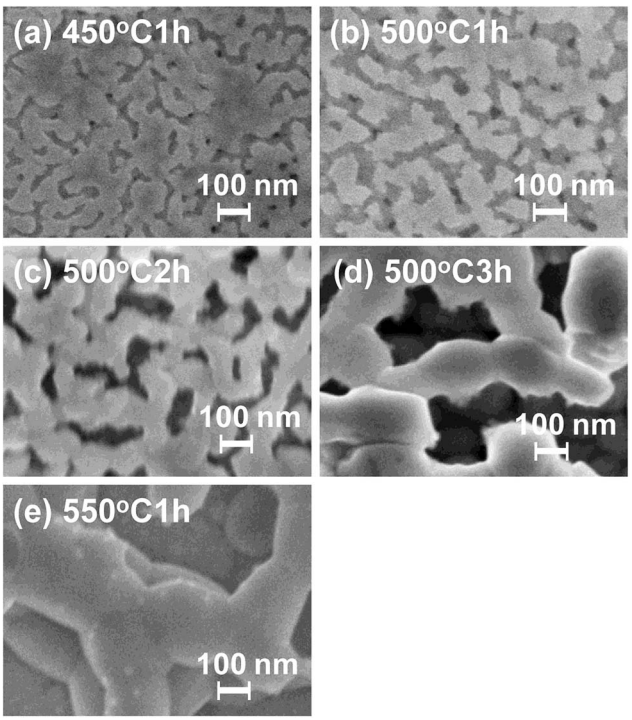

Fig. 3 The surface SEM images of $BiVO_4$ electrodes (4-coat) prepared by coating an aqueous Bi and V solution (pH 7) onto an ITO glass substrate (1.25 × 1.25 cm^2), followed by drying (65 °C) and calcination at 450, 500 and 550 °C for 1–3 h.

a diameter of smaller than 100 nm (Fig. 3(a) and (b)), while the sample calcined at 550 °C (Fig. 3(e)) was composed of larger particles with a diameter of *ca.* 200 nm.

The photoanode fabricated in this study has 3D-porous network structure as observed with $BiVO_4$ photoanode reported by Kim and Choi; however, the particle size of our $BiVO_4$ film (primary particle size: <100 nm) is smaller than that of their film (primary particle size: >100 nm).[12] To the best of our knowledge, our report is the first example of $BiVO_4$ film with porous network structure consisting of such small particles. The particle sizes also increased as the calcinations time increased when compared at the same calcination temperature (see Fig. 3(b)–(d) and S3†). In contrast, $BiVO_4$ films that were prepared using aqueous precursor solutions of various pH values (pH 4–9) were consisted of $BiVO_4$ particles with the same s–m structure and similar particle size (<100 nm) (Fig. 2 and S4†), presumably due to the use of appropriate ligands that effectively stabilize metal ions in the aqueous solution at wide range of pH.

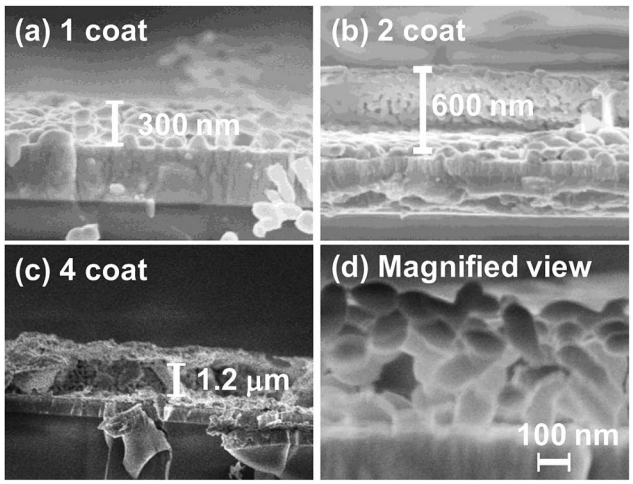

Fig. 4 (a–c) Cross-sectional SEM images of $BiVO_4$ electrodes with different coating times. (d) Magnified view of cross-sectional SEM images of $BiVO_4$ electrodes (1 coat-500 °C-1 h).

The cross-sectional SEM analysis revealed that the film thickness of *n*-coated-500 °C-1 h ($n = 1$ to 5) were about *ca.* 300, 600 and 900 nm, and 1.2 and 1.5 μm, respectively (Fig. 4 and S4†). Thus, the film thickness constantly increased by *ca.* 300 nm with increasing numbers of the coating repetition (see Fig. 4 and S5†). In addition, the magnified view of the cross-sectional images clearly showed that the $BiVO_4$ film had porous structures with an aggregated network of particles (Fig. 4(d)). As described above, the simple coating of aqueous Bi and V solutions containing EDTA and tart is capable of providing porous nanoparticulate $BiVO_4$ films with controllable thickness.

PEC properties of $BiVO_4$ photoelectrodes for sulfite oxidation under simulated solar-light

In order to examine the ability of $BiVO_4$ photoelectrodes prepared under various conditions, the PEC properties of the photoanodes were assessed in an electrolyte solution containing 0.2 M Na_2SO_3 as a hole scavenger. Typical *J–V* curves for sulfite oxidation over the $BiVO_4$ films are shown in Fig. 5. All the $BiVO_4$ electrodes exhibited obvious photo-response under simulated sunlight irradiation. The photocurrents depended on the preparation conditions, while the onset potentials were

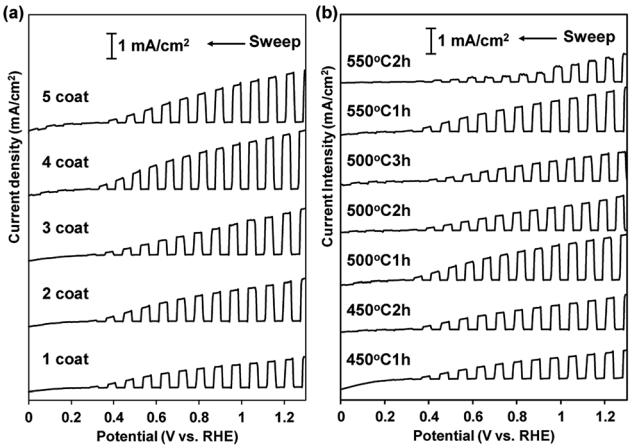

Fig. 5 (a) *J–V* curves of nanoporous $BiVO_4$ electrodes for sulfite oxidation. (a) Samples with different coating times. (b) Samples prepared under different calcination conditions (450–550 °C for 1–3 hours). Conditions: in a 0.2 M phosphate buffer (pH 7) containing 0.2 M Na_2SO_3 as hole scavenger under AM 1.5 G, 100 mW cm^{-2} illumination (scan rate, 10 mV s^{-1}).

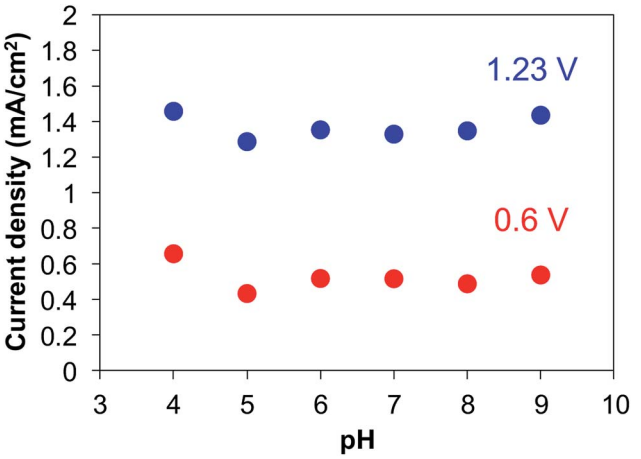

Fig. 6 Effect of the pH value of precursor solutions on the anodic photocurrent density of $BiVO_4$ electrodes. PEC measurement was carried out in a 0.2 M phosphate buffer (pH 7) containing 0.2 M Na_2SO_3 as hole scavenger under AM 1.5 G, 100 mW cm^{-2} illumination (scan rate, 10 mV s^{-1}).

located at about 0.3 V *vs.* RHE with all samples. In the case of changing numbers of coating repetition, the photocurrent increased with increasing numbers of coating repetition up to fourth cycles (1.4 mA at 1.23 V *vs.* RHE) and saturated at the fifth coating cycle (Fig. 5(a)).

As described above, the film thickness increased with increasing number of coating. The results suggest that almost all of the particles in the films effectively can absorb the light up to *ca.* 1 μm in thickness. The photocurrent was also dependent on the calcination conditions (temperature and time); the highest photocurrent was observed with the sample calcined at 500 °C for 1 h (Fig. 5(b)). The highest current density of the sample calcined at 500 °C for 1 h is certainly due to the balance of good crystallinity and high specific surface area of the particles. In contrast, the photocurrent density was not affected by the pH value of the precursor solutions (see Fig. 6, summarized the photocurrent at 0.6 and 1.23 V *vs.* RHE), which is in agreement with the observation that the film morphology did not depend on the pH value of the precursor solutions (*vide supra*).

PEC properties of $BiVO_4$ photoelectrodes for water oxidation under simulated solar-light

We next examined water oxidation by the $BiVO_4$ photoelectrodes. As an effective co-catalyst for water oxidation, small amounts of CoPi were electrochemically deposited on the $BiVO_4$ photoelectrodes.[8] The top view SEM elemental mapping images (SEM-EDX) of the surface of CoPi-loaded $BiVO_4$ photoanode (4 coat-500 °C-1 h) indicate homogeneous loading of Co species (see Fig. S6†). Fig. 7 shows the *J–V* curves of the CoPi-loaded $BiVO_4$ photoelectrodes (4-coated-500 °C-1 h) prepared using precursor solutions at pH 3, 7 and 9, which exhibited the best PEC performance for sulfite oxidation. The onset potential of CoPi-loaded $BiVO_4$ photoelectrodes was more negative than that observed with bare $BiVO_4$ sample, which is in agreement with the report with CoPi-loaded $BiVO_4$ photoelectrodes by van de Krol and coworkers.[10] The CoPi-loaded $BiVO_4$ photoelectrodes showed a photocurrent density of *ca.* 1.5 mA cm^{-2} at 1.23 V *vs.* RHE for water oxidation, which was higher anodic photocurrent than that of bare $BiVO_4$ sample (Fig. 7). The value of photocurrent on present CoPi-loaded $BiVO_4$ photoanode does not reach the high value reported by Kim and Choi (*ca.* 5.0 mA cm^{-2} at 1.23 V *vs.* RHE);[12] however, the value was higher than that reported with $BiVO_4$ anodes prepared by using highly-acidic aqueous precursor solutions (<0.5 mA cm^{-2} at 1.23 V *vs.*

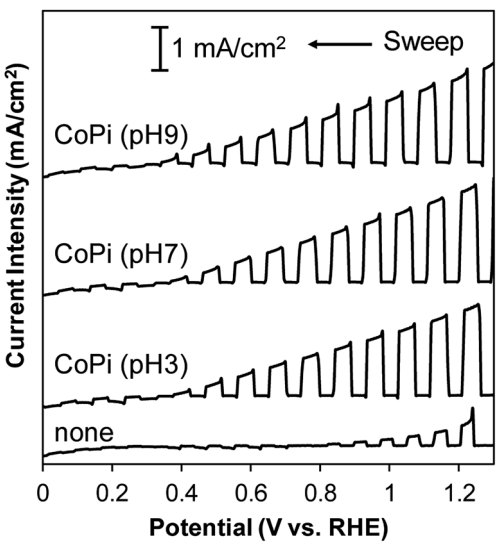

Fig. 7 *J–V* curves of CoPi-loaded $BiVO_4$ electrode (4-coated-500 °C-1 h) prepared from an aqueous Bi and V precursor solution of different pH, and $BiVO_4$ electrode without CoPi loading (4-coated-500 °C-1 h) prepared from an aqueous Bi and V precursor solution of pH 7 for water oxidation measured in a 0.2 M phosphate buffer (pH 7) under AM 1.5 G, 100 mW cm^{-2} illumination (scan rate, 10 mV s^{-1}).

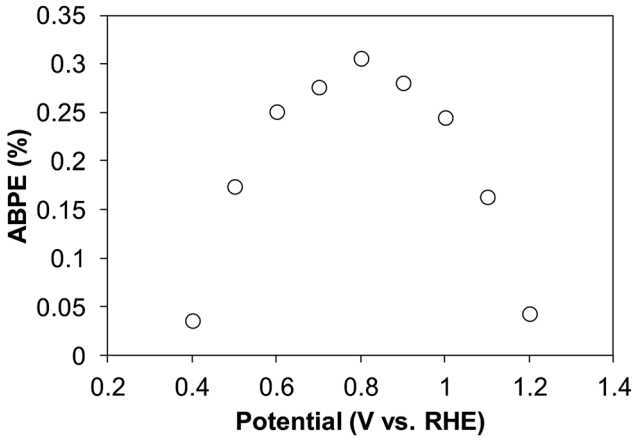

Fig. 8 ABPE plots calculated by using CoPi-loaded $BiVO_4$ photoanode (4-coated-500 °C-1 h) prepared from a precursor solution of pH 7 under simulated sunlight irradiation.

RHE).[18,24] The observed relatively high performance should be attributed to the appropriate porous nanoparticulate structure and contact interface. The 3D structure should be attained by direct particle growth from precursor solution on the ITO substrate.

We also examined the stability of $BiVO_4$ photoanodes with/without CoPi loading. It has been reported that CoPi is stable at pH > 6.[31] Therefore, we conducted the stability test at pH 7 and 8. Fig. S7† shows the amperometric *J–t* curves of $BiVO_4$ photoanodes with/without CoPi loading at pH 7 and 8 under continuous illumination at 0.8 V *vs.* RHE. CoPi-loaded $BiVO_4$ photoanode exhibited better stability at pH 8 than at pH 7; however, about 50% of the initial photocurrent was retained for CoPi-loaded $BiVO_4$ in the phosphate electrolyte of pH 8 after 2 h illumination (Fig. S7(a)†). In contrast, the $BiVO_4$ photoanode without co-catalyst loading (Fig. S7(b)†) did not show significant pH dependence of photocurrent decay, and more than 80% of the beginning current was retained after 2 h light irradiation. Thus, the photocurrent decay of CoPi-loaded $BiVO_4$ photoanode suggests the instability of CoPi, rather than $BiVO_4$ itself. The stability of the present CoPi-loaded $BiVO_4$ photoanode is not sufficiently high; however, there are some possibilities to improve the stability by loading other co-catalysts.[32–34]

The applied bias photon-to-current efficiency (ABPE) was calculated for the CoPi-loaded $BiVO_4$ photoelectrodes (4-coated-500 °C-1 h) under simulated sunlight irradiation (100 mW cm^{-2}) using the following equation.

$$\text{ABPE (\%)} = 100 \times [\text{photocurrent/mA cm}^{-2}] \times [(1.23 - V_{\text{RHE}})/\text{V}]/[\text{photon flux/mW cm}^{-2}]$$

In the range of 0.4 V to 1.2 V *vs.* RHE, the CoPi-loaded $BiVO_4$ photoelectrode gave the highest ABPE of 0.31% at 0.8 V *vs.* RHE under simulated sunlight irradiation (Fig. 8). Thus, highly efficient photoelectrodes for water oxidation can be fabricated by drop-casting aqueous metal precursors and calcination under environmentally friendly conditions.

Conclusions

In summary, $BiVO_4$ photoanodes were directly fabricated onto ITO substrates by drop-casting using aqueous Bi and V solutions containing EDTA and tart. The chelators stabilize the precursor solutions in a wide range of pH. It should be noted that the procedure described here possesses numbers of desirable properties; no use of organic solvents, neutral pH, and easy process to yield nanoporous $BiVO_4$ films. Especially, it is possible to prepare $BiVO_4$ films with the same structure at a wide range of pH if our aqueous precursor solutions are employed, which would be a great benefit to many researchers in this field. The essence of our present fabrication approach using aqueous chelating solutions is expected to be widely applicable to the preparation of other metal oxide films.

Conflicts of interest

There are no conflicts to declare.

Notes and references

1 A. Fujishima and K. Honda, *Nature*, 1972, **238**, 37–38.
2 K. Maeda and K. Domen, *J. Phys. Chem. C*, 2007, **111**, 7851–7861.
3 R. Abe, *J. Photochem. Photobiol., C*, 2010, **11**, 179–209.
4 F. E. Osterloh, *Chem. Soc. Rev.*, 2013, **42**, 2294–2320.
5 A. Kudo, K. Ueda, H. Kato and I. Mikami, *Catal. Lett.*, 1998, **53**, 229–230.
6 H. Liu, R. Nakamura and Y. Nakato, *J. Electrochem. Soc.*, 2005, **152**, G856–G861.
7 K. Sayama, A. Nomura, T. Arai, T. Sugita, R. Abe, M. Yanagida, T. Oi, Y. Iwasaki, Y. Abe and H. Sugihara, *J. Phys. Chem. B*, 2006, **110**, 11352–11360.
8 D. K. Zhong, S. Choi and D. R. Gamelin, *J. Am. Chem. Soc.*, 2011, **133**, 18370–18377.
9 Q. Jia, K. Iwashina and A. Kudo, *Proc. Natl. Acad. Sci. U. S. A.*, 2012, **109**, 11564–11569.
10 F. F. Abdi, N. Firet and R. van de Krol, *ChemCatChem*, 2013, **5**, 490–496.
11 Y. Park, K. J. McDonald and K. S. Choi, *Chem. Soc. Rev.*, 2013, **42**, 2321–2337.
12 T. Kim and K. S. Choi, *Science*, 2014, **343**, 990–994.
13 W. He, R. Wang, L. Zhang, J. Zhu, X. Xiang and F. Li, *J. Mater. Chem. A*, 2015, **3**, 17977–17982.
14 W. He, R. Wang, C. Zhou, J. Yang, F. Li and X. Xiang, *Ind. Eng. Chem. Res.*, 2015, **54**, 10723–10730.
15 Y. Tang, R. Wang, Y. Yang, D. Yan and X. Xiang, *ACS Appl. Mater. Interfaces*, 2016, **8**, 19446–19455.
16 J. H. Kim, Y. H. Jo, J. H. Kim and J. S. Lee, *Nanoscale*, 2016, **8**, 17623–17631.
17 Y. Kuang, Q. Jia, H. Nishiyama, T. Yamada, A. Kudo and K. Domen, *Adv. Energy Mater.*, 2016, **6**, 1501645.

18 A. Iwase, S. Ikeda and A. Kudo, *Chem. Lett.*, 2017, **46**, 651–654.
19 Y. Kuang, T. Yamada and K. Domen, *Joule*, 2017, **1**, 290–305.
20 M. Rohloff, B. Anke, S. Zhang, U. Gernert, C. Scheu, M. Lerch and A. Fischer, *Sustainable Energy Fuels*, 2017, **1**, 1830–1846.
21 K. R. Tolod, S. Hernández and N. Russo, *Catalysts*, 2017, **7**, 13, DOI: 10.3390/catal7010013.
22 X. Zhang, R. Wang, F. Li, Z. An, M. Pu and X. Xiang, *Ind. Eng. Chem. Res.*, 2017, **56**, 10711–10719.
23 J. H. Baek, B. J. Kim, G. S. Han, S. W. Hwang, D. R. Kim, I. S. Cho and H. S. Jung, *ACS Appl. Mater. Interfaces*, 2017, **9**, 1479–1487.
24 A. Iwase, S. Nozawa, S. I. Adachi and A. Kudo, *J. Photochem. Photobiol., A*, 2018, **353**, 284–291.
25 G. Park, J. Y. Park, J. H. Seo, K. H. Oh, A. Ma and K. M. Nam, *Chem. Commun.*, 2018, **54**, 5570–5573.
26 R. Wang, L. Luo, X. Zhu, Y. Yan, B. Zhang, X. Xiang and J. He, *ACS Appl. Energy Mater.*, 2018, **1**, 3577–3586.
27 H. S. Han, S. Shin, D. H. Kim, I. J. Park, J. S. Kim, P. S. Huang, J. K. Lee, I. S. Cho and X. Zheng, *Energy Environ. Sci.*, 2018, **11**, 1299–1306.
28 S. Okunaka, H. Tokudome, Y. Hitomi and R. Abe, *J. Mater. Chem. A*, 2016, **4**, 3926–3932.
29 A. Kudo, K. Omori and H. Kato, *J. Am. Chem. Soc.*, 1999, **121**, 11459–11467.
30 S. M. Thalluri, C. Martinez Suarez, M. Hussain, S. Hernandez, A. Virga, G. Saracco and N. Russo, *Ind. Eng. Chem. Res.*, 2013, **52**, 17414–17418.
31 Y. Surendranath, D. A. Lutterman, Y. Liu and D. G. Nocera, *J. Am. Chem. Soc.*, 2012, **134**, 6326–6336.
32 D. Wang, R. Li, J. Zhu, J. Shi, J. Han, X. Zong and C. Li, *J. Phys. Chem. C*, 2012, **116**, 5082–5089.
33 J. Yang, D. Wang, H. Han and C. Li, *Acc. Chem. Res.*, 2013, **46**, 1900–1909.
34 D. K. Lee and K. S. Choi, *Nat. Energy*, 2018, **3**, 53–60.